International Journal of Infectious Diseases 17 (2013) e539–e545

Contents lists available at SciVerse ScienceDirect

International Journal of Infectious Diseases

journal homepage: www.elsevier.com/locate/ijid

Hepatitis C virus core protein induces hepatic metabolism disorders through down-regulation of the SIRT1–AMPK signaling pathway

Jian-Wu Yu [a], Li-Jie Sun [a,*], Wei Liu [b], Yong-Hua Zhao [a], Peng Kang [a], Bing-Zhu Yan [a]

[a] Department of Infectious Diseases, Second Affiliated Hospital, Harbin Medical University, 246 Xuefu Road, Nangang District, Harbin 150086, China
[b] Scientific Research and Experimental Center, Second Affiliated Hospital, Harbin Medical University, Harbin, China

ARTICLE INFO

Article history:
Received 29 August 2012
Received in revised form 17 December 2012
Accepted 31 January 2013

Corresponding Editor: Eskild Petersen, Aarhus, Denmark

Keywords:
Hepatitis C viruses
Core protein
Hepatic glucose metabolism
Hepatic lipid metabolism
SIRT1
AMPK

SUMMARY

Background: Steatosis and insulin resistance induced by hepatitis C virus (HCV) infection are, at least in part, critical factors for the progression of chronic hepatitis C (CHC) and can influence the outcome of antiviral treatment. Silent information regulator 1 (SIRT1) and adenosine monophosphate-activated protein kinase (AMPK) play a key role in the regulation of hepatic glucose and lipid metabolism. The aim of this study was to investigate the possible effect of HCV core protein on energy, glucose, and lipid metabolism of hepatocytes and expression of SIRT1 and AMPK.

Methods: HCV core protein expression plasmid was transfected into HepG2 cells. The level of reactive oxygen species (ROS) and values of NAD^+/NADH and ATP/ADP were detected. Intracellular levels of triacylglycerol (TG), cholesterol, glucose uptake by hepatocytes, and glucose production were measured. The expression levels of mRNA and protein of SIRT1 and AMPK were detected. The mRNA levels of SIRT1 and AMPK downstream glucose and lipid metabolism genes were measured.

Results: In HepG2 cells expressing HCV core protein, the level of ROS increased, the value of NAD^+/NADH decreased, the activity and expression levels of mRNA and protein of SIRT1 and AMPK decreased, glucose uptake and its regulator gene GLUT2 mRNA levels decreased, glucose production and its regulator genes PEPCK and G6Pase mRNA levels increased, intracellular TG and cholesterol contents and their regulator gene (SREBP-1c, FAS, ACC, HMGR, and HMGS) mRNA levels increased, the glycolytic gene GK and fatty acid oxidation genes PPARα and CPT1A mRNA levels decreased.

Conclusions: HCV core protein induces alterations in cellular redox state (decrease in the NAD^+/NADH ratio), which could influence the activity of SIRT1 and secondarily AMPK, then change the expression profile of glucose and lipid metabolism-related genes, thereby causing metabolism disorders of hepatocytes.

1. Introduction

Chronic hepatitis C virus (HCV) infection is often associated with insulin resistance and hepatic steatosis. Insulin resistance has been implicated in the progression of fibrosis and cirrhosis and the development of diabetes in chronic hepatitis C (CHC) infection. In a previous study we demonstrated that insulin resistance and hyperinsulinemia adversely affected the virological response rates to anti-HCV therapy,[1] and a combination of adenosine monophosphate-activated protein kinase (AMPK) activator metformin, pegylated interferon α2a (PEG-IFNα2a), and ribavirin improved insulin sensitivity and increased the sustained virologic response (SVR) rate with a good safety profile.[2] However, the mechanism underlying these phenomena is not yet fully understood.

AMPK is a major cellular energy sensor that is activated by cellular stresses that increase intracellular AMP. In addition to allosteric regulation by AMP, AMPK is regulated by AMPK kinases such as proteins LKB1.[3] Activated AMPK augments fatty acid oxidation and decreases glucose output and cholesterol and triglyceride (TG) synthesis in hepatocytes.[4,5] Only a few studies on the interaction between AMPK and HCV infection have been reported. It has been stated that HCV infection causes Ser485/491 phosphorylation of AMPK and inhibits the kinase activity of AMPK and increases lipid accumulation, facilitating HCV replication.[6] As suggested in a recent study,[7] a low glucose concentration inhibits HCV replication along with activation of AMPK, treatment with AMPK activator suppresses HCV replication, and AMPK inhibitor has the opposite effect.

Silent information regulator 1 (SIRT1) is a nicotinamide adenine dinucleotide (NAD^+)-dependent histone deacetylase, and it acts as a modulator of cellular metabolism under different physiological conditions. Modifications in NAD^+ levels are likely to be the most

* Corresponding author. Tel./Fax: +86 0451 86605614.
E-mail address: lijiesun5234@yahoo.com.cn (L.-J. Sun).

1201-9712/$36.00 – see front matter © 2013 International Society for Infectious Diseases. Published by Elsevier Ltd. All rights reserved.
http://dx.doi.org/10.1016/j.ijid.2013.01.027

important regulators of SIRT1 activity.[8] AMPK and SIRT1 interact with each other. Changes in AMPK activity are associated with alterations in SIRT1 abundance and activity. SIRT1 activation and inhibition by pharmacological agents produce parallel changes in AMPK.[9]

A considerable number of studies have also suggested that HCV core protein leads to energy, glucose, and lipid metabolic disorders.[10–12] However, the precise mechanisms are poorly understood. The role of the SIRT1–AMPK signal pathway has become a research hotspot for elucidating the mechanism of diabetes and alcoholic liver disease. Due to the close associations between chronic HCV infection and diabetes, we speculated that the SIRT1–AMPK signal pathway may play an important role in hepatic metabolism disorders caused by HCV infection. Utilizing HepG2 cells expressing HCV core protein, we studied the effect of HCV core protein on SIRT1 and AMPK, and their downstream glucose and lipid metabolism-related genes, as well as energy, glucose, and lipid metabolism of hepatocytes.

2. Materials and methods

2.1. Cell culture

HepG2 cells were cultured in Dulbecco's modified Eagle's medium (DMEM) (Hyclone, Logan, UT, USA) containing 10% fetal bovine serum (FBS) (Hyclone), 100 U/ml penicillin (Hyclone), 100 μg/ml streptomycin (Hyclone), and 5.5 mM D-glucose. The cells were incubated in a humidified atmosphere of 5% CO_2 at 37 °C and passaged every 3 days by trypsinization.

2.2. Transfections

For transfections, HepG2 cells were used at a confluency of 50–60%. Approximately 5×10^5 HepG2 cells were seeded into six-well tissue culture plates at 24 h prior to transfection. HepG2 cells were transfected with 2 μg of pcDNA3.1(−)-core (containing the full-length HCV core gene, kindly provided by Prof. Jun Cheng, Beijing Titan Hospital, Beijing) or pcDNA3.1(−) (Invitrogen, Carlsbad, CA, USA) in Opti-MEM (Invitrogen) using Lipofectamine 2000 (Invitrogen) in accordance with the manufacturer's protocol. After 6 h incubation at 37 °C in 5% CO_2, the cells were washed with 1× phosphate-buffered saline (PBS) and DMEM with serum was added to the cells. After 48 h of transfection, cells were treated with G418 (500 μg/ml). Following selection for 2 weeks, total populations of G418-resistant cells were pooled and single-cell sorted into 96-well plates with a growth medium containing 500 μg/ml G418. Sorted single cells were grown under selection for an additional 2 weeks and expanded into stable cell lines. Cells were harvested for HCV core gene expression analysis by Western blot analysis. In this study, HepG2 cells transfected with empty vectors (pcDNA3.1(−)) were used as control.

2.3. Determination of reactive oxygen species

Cells were plated onto glass coverslips and examined for reactive oxygen species (ROS) production as a marker for oxidative stress. They were loaded for 2 h with chloromethyl 2′,7′-dichlorodihydrofluorescein diacetate (Molecular Probes Inc., Eugene, OR, USA) at a final concentration of 10 μmol/l.[13] The incorporated radioactivity was measured by liquid scintillation counter (LS6500; Beckman Coulter, Fullerton, CA, USA). Results were expressed as relative fluorescence intensity and normalized to the control cells.

2.4. ATP/ADP ratio

The adenosine triphosphate (ATP)/adenosine diphosphate (ADP) ratio was measured using the ApoSENSOR ADP/ATP Ratio Assay (Biovision, CA, USA) following the manufacturer's instructions. One hundred microliters of reaction mix (5 μl ATP monitoring enzyme, 95 μl nucleotide-releasing buffer) was added to the appropriate wells of a 96-well plate for 6 h to burn off low-level ATP contamination, then the background luminescence was read. Ten thousand cells were treated with 50 μl of nucleotide-releasing buffer for 5 min at room temperature with gentle shaking and transferred to a luminometer plate. ATP levels in the sample cells were measured in a beta counter after 10 min (data A). ADP levels were measured after 10 min (data B), then 1 μl ADP-converting enzyme was added, and the sample was measured again after 10 min (data C). The ATP/ADP ratio was calculated as: data A/(data C − data B).

2.5. NAD^+/NADH ratio

The NAD^+/NADH ratio was measured using the NAD^+/NADH Quantification Kit (Biovision). NAD^+ was extracted from the cell pellet by adding 7% perchloric acid with sonication on ice for 5 min. The sample was centrifuged for 3 min at room temperature and neutralized with 1 M phosphate buffer and 3 M NaOH solution. The clear supernatant was mixed with the cycling buffer containing 25 mM Tris–HCl (approximately pH 8), 5 mM $MgCl_2$, 50 mM KCl, 2.25 mM lactate, 54 μM resazurin, and 36 U/ml of diaphorase. The cycling reaction was initiated with the addition of lactate dehydrogenase and the increase in the resorufin fluorescence (with excitation at 560 nm and emission at 590 nm) was measured continuously using a fluorescent plate reader. NADH was extracted from cell pellet by adding 0.05 M NaOH/1 mM ethylenediaminetetraacetic acid (EDTA) with sonication on ice for 5 min. The alkali extract was incubated at 60 °C for 30 min and neutralized with 0.1 M HCl and 300 mM phosphate buffer (approximately pH 4.4). The concentration of NADH was measured fluorometrically using the cycling assay described above. Standard curves were obtained by processing the standard NAD^+ and NADH samples described above.

2.6. Measurement of SIRT1 activity

SIRT1 activity was measured using a SIRT1 fluorometric assay kit (BIOMOL, Plymouth Meeting, PA, USA) in accordance with the manufacturer's instructions, with slight modifications.[14] A 25-μl volume of cell extracts was incubated with 15 μl of Fluor de Lys-SIRT1 substrate (100 μM) and NAD^+ (100 μM) for 30 min at 37 °C. The reaction was stopped by the addition of 50 ml of developer reagent and nicotinamide (2 mM), and the fluorescence was subsequently monitored for 30 min at 360 nm (excitation) and 460 nm (emission). Experimental values were recorded as pmol converted substrate/μg protein/min. Data were recorded as values relative to those for mock-transfected HepG2 cells.

2.7. Measurement of AMPKα2 activity

AMPK activity was measured as previously described.[15] Briefly, cell lysates (150 μg protein) were immunoprecipitated with specific antibodies against α2 catalytic subunits of AMPK (Bethyl Laboratories, Montgomery, TX, USA). The kinase reaction was carried out in 40 mmol/l HEPES (pH 7.0), 0.1 mmol/l synthetic SAMS peptide, 0.2 mmol/l AMP, 80 mmol/l NaCl, 0.8 mmol/l dithiothreitol, 5 mmol/l $MgCl_2$, and 0.2 mmol/l ATP (2 μCi of [γ-32P]ATP) for 20 min at 30 °C. Reaction products were spotted on Whatman P81 filter paper, the papers were extensively washed in

1% phosphoric acid, and radioactivity was assessed with a scintillation counter. Kinase activity was assessed by incorporated ATP (pmol) per immunoprecipitated protein (mg) per min. Data were recorded as values relative to those for mock-transfected HepG2 cells.

2.8. Glucose uptake by hepatocytes

Cells were cultured in a 12-well plate for the glucose uptake assay. After serum starvation overnight in 0.1% bovine serum albumin–DMEM, the cells were subsequently incubated in 1 ml of PBS containing 100 nM insulin for 30 min at 37 °C. After being washed with PBS, cells were incubated in 1 ml of PBS containing 1 μCi of 2-deoxy-D-[3H]-glucose/ml (Amersham Life Sciences, Buckinghamshire, UK) for 5 min. The reaction was stopped by adding 0.1 mM cytochalasin B on ice. The cells were washed with ice-cold PBS and solubilized in 0.4 ml of NaOH (0.05 M). The incorporated radioactivity was measured in 4 ml of scintillation fluid by liquid scintillation counter.

2.9. Glucose production assay

Culture medium was replaced with glucose production buffer consisting of glucose-free DMEM, without phenol red, supplemented with a gluconeogenic substrate (2 mM sodium pyruvate and 20 mM sodium lactate). After 24 h of incubation, the medium was collected, and the total glucose concentration was measured using a commercial kit (Glucose CII Test Wako, Wako Pure Chemical Industries, Osaka, Japan) and normalized to the cellular protein content. As the baseline of glucose production, glucose-free DMEM with neither sodium pyruvate nor sodium lactate was used. Glucose production via gluconeogenesis equals the total glucose production minus the baseline glucose production. The data recorded were the means of six independent experiments, and the value for the control cells was arbitrarily expressed as 1.0.

2.10. Measurement of triglyceride and cholesterol content

Cells were maintained in serum-free medium overnight. After the medium was removed, the cells were washed three times with PBS and resuspended in 200 μl of PBS. Then lipids were extracted from 100 μl of PBS by the method of Bligh and Dyer[16] and resuspended in 100 μl of 10% Triton X. The cellular contents of TG and cholesterol were measured using enzyme reagents (Wako). TG and total cholesterol contents were expressed as μg of lipid/mg of cellular protein.

2.11. Real-time PCR analysis for SIRT1, AMPKα2, and glucose and lipid metabolism-related gene mRNA levels

Total cellular RNA was isolated using the TRIzol reagent (Invitrogen) following the supplier's protocol. cDNA was generated using Quanti Tect Reverse Transcription system (Qiagen, Valencia, CA, USA). Real-time quantitative PCR was performed on a SYBR Premix Ex Taq (Takara Bio, Kyoto, Japan) using SYBR green chemistry in an ABI PRISM 7000 (Applied Biosystems, Foster, CA, USA). Glyceraldehyde-3-phosphate dehydrogenase (GAPDH) was used as internal control for normalization. The PCR primers for the amplification of SIRT1, AMPKα2, glucose transporter 1 (GLUT1), GLUT2, glucokinase (GK), phosphoenolpyruvate carboxykinase (PEPCK), glucose-6-phosphatase (G6Pase), sterol regulatory element binding protein (SREBP)-1c, SREBP-2, HMG-CoA reductase (HMGR), HMG-CoA synthase (HMGS), peroxisome proliferator-activating receptor (PPAR)α, PPARγ, acetyl-coenzyme A carboxylase (ACC), fatty acid synthesis<!– (FAS), carnitine palmitoyl transferase-1 (CPT1), and GAPDH are listed in Table 1. PCR conditions were as follows: 95 °C for 30 s, 58 °C for 30 s, and extension at 72 °C for 45 s, 40 cycles. The relative gene expression analysis was carried out using SDS 3.1 software (Applied Biosystems).

2.12. Western blot

Cells were lysed in buffer (20 mM Tris–HCl, pH 8.0, 1% Nonidet P-40, 1 mM EDTA, 1 mM ethylene glycol tetraacetic acid (EGTA), 1 mM sodium orthovanadate, 1 mM dithiothreitol, 1 mM phenylmethylsulfonyl fluoride, 2 μg/ml aprotinin, 2 μg/ml leupeptin, and 1 μg/ml pepstatin). Cell debris was removed by centrifugation at 14 000 × *g* for 15 min at 4 °C, and the cell supernatant was used for Western blotting. Protein quantification was carried out using a bicinchoninic acid protein assay kit (Thermo Fisher Scientific, Rockford, IL, USA). Fifty micrograms of protein was separated by 8% sodium dodecyl sulfate polyacrylamide gel electrophoresis (SDS-PAGE) and electrophoretically transferred to a polyvinylidene difluoride transfer membrane (Millipore, Billerica, MA, USA). The membranes were blocked with 5% nonfat dry milk in Tris-buffered

Table 1
Sequences of primers used for the real-time polymerase chain reaction

Genes	Forward 5′–3′	Reverse 5′–3′	PCR product (bp)
SIRT1	CGGAAACAATACCTCCACCTGA	GAAGTCTACAGCAAGGCGAGCA	242
SREBP-2	ACAACCCATAATATCATTGAGAAACG	TTGTGCATCTTGGCGTCTGT	100
HMGR	GCCTGGCTCGAAACATCTGAA	CTGACCTGGACTGGAAACGGATA	135
HMGS	GTATGCCCTGGTAGTTGCAGGAG	TGTTGCATATGTGTCCCACGAA	146
AMPKα2	AGCATGGACGGGTTGAAGAG	GTGGCGACAGAACGATTGAG	409
GLUT1	TGAACCTGCTGGCCTTC	GCAGCTTCTTTAGCACA	399
GLUT2	TGG GCTGAGGAAGAGACTGT	AGAGACTGAAGGATGGCTCG	461
SREBP-1c	CTTTGCCCACCCTGGTGAGT	GGTTCTCCTGCTTGAGTTTCTGG	315
PPARα	GACGTGC TTCCTGCTTCATAGA	CCACCATCGCGACCAGAT	374
FAS	GAAACTGCAGGAGC TGTC	CACGGAGTTGAGGCGGAT	285
ACC	GCTGCTCGGATCACTAGTGAA	TTCTGCTATCAGTCTGTCCAG	338
PPAR γ	GAAATGACCATGGTTGAC	CCGCTAGTACAAGTCCTTGTA	437
GK	GCCTCCCAAAGCATCTACCTC	GCTCCACTG CCCCTCCTCACC	444
G6Pase	CCTGGGGCTGGCTCTCAACTC	AATAGTAGTCCTC CTCAATCC	309
PEPCK	CCAGGCAGTGAGGGAGTTTCT	ACTGTGTCTCTTTGCTCTTGG	217
GAPDH	GACAACTTTGGCATCGT	ATGCAGGGATGATGTTCTGG	133
CPT1A	AGACGGTGGAACAGAGGCTGAA	TGAGACCAAACAAAGTGATGATGTCAG	102

SIRT, silent information regulator; SREBP, sterol regulatory element binding protein; HMGR, HMG-CoA reductase; HMGS, HMG-CoA synthase; AMPK, AMP-activated protein kinase; GLUT, glucose transporter; PPAR, peroxisome proliferator-activating receptor; FAS, fatty acid synthase; ACC, acetyl-coenzyme A carboxylase; GK, glucokinase; G6Pase, glucose 6-phosphatase; PEPCK, phosphoenolpyruvate carboxykinase; GAPDH, glyceraldehyde-3-phosphate dehydrogenase; CPT1A, carnitine palmitoyl transferase 1.

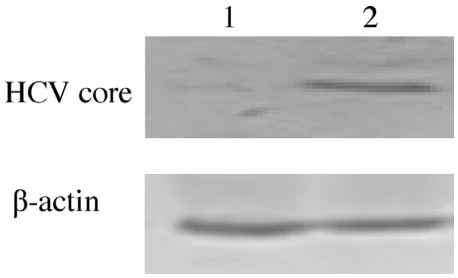

Figure 1. The expression of HCV core protein by Western blot; 1, mock-transfected HepG2 cells; 2, HepG2 cells expressing the HCV core protein.

saline with 0.1% Tween 20 and incubated with specific antibodies (anti-phospho-AMPKα (Thr172) monoclonal antibody, anti-AMPKα antibody (Cell Signaling Technologies, Beverly, MA, USA), anti-SIRT1 antibody, anti-HCV core monoclonal antibody (Santa Cruz Biotechnology, Santa Cruz, CA, USA)), followed by incubation with horseradish peroxidase-conjugated goat anti-mouse IgG or goat anti-rabbit IgG (Santa Cruz Biotechnology). The respective protein bands were visualized with an enhanced chemiluminescence detection system (Perkin Elmer, Waltham, MA,USA). Protein loading was normalized by probing with anti-GAPDH monoclonal antibody (Millipore).

2.13. Statistical analysis

Results are expressed as the mean ± standard deviation. Significance was determined using the Student's *t*-test, and statistical significance was defined as $p < 0.05$.

3. Results

3.1. Expression of HCV core protein

HCV core protein was detected in HepG2 cells expressing HCV core protein by Western blot, and not detected in mock-transfected HepG2 cells (Figure 1).

3.2. Effect of HCV core protein on energy metabolism of hepatocytes

Compared to mock-transfected HepG2 cells, the level of ROS in HepG2 cells expressing HCV core protein significantly increased (4 ± 0.5 vs. 1 ± 0.1; $t = 14.411$, $p < 0.01$) (Figure 2a), and the value of NAD^+/NADH decreased (0.02 ± 0.005 vs. 0.08 ± 0.02; $t = 7.348$, $p < 0.01$) (Figure 2b). There was no difference in the value of ATP/ADP between the two cell populations (9.3 ± 2.8 vs. 8.2 ± 2.2; $t = 0.757$, $p > 0.05$) (Figure 2a).

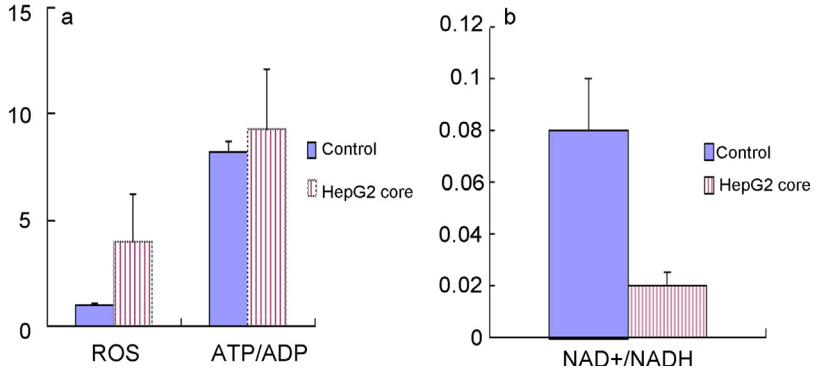

Figure 2. Effect of HCV core protein on energy metabolism of hepatocytes. The ROS level, ATP/ADP ratio, and NAD^+/NADH ratio were assayed as described in the Materials and methods section. The data shown are the means of six independent experiments (abbreviations: ROS, reactive oxygen species; ATP, adenosine triphosphate; ADP, adenosine diphosphate; NADH, nicotinamide adenine dinucleotide).

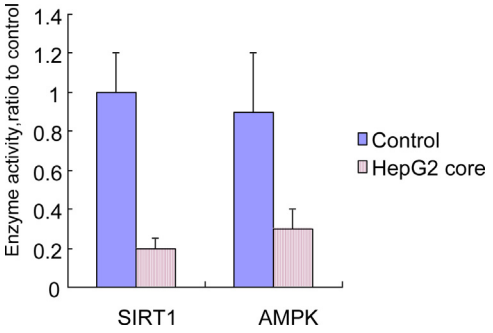

Figure 3. Effect of HCV core protein on activity of SIRT1 and AMPK. The activity of SIRT1 and AMPK was assayed as described in the Materials and methods section. The data shown are the means of six independent experiments (abbreviations: SIRT1, silent information regulator 1; AMPK, AMP-activated protein kinase).

3.3. Effect of HCV core protein on activity and expression of SIRT1

Compared to mock-transfected HepG2 cells, the activity of SIRT1 (0.2 ± 0.05 vs. 1.0 ± 0.2, $t = 9.505$, $p < 0.01$) in HepG2 cells expressing HCV core protein decreased (Figure 3); the mRNA levels of SIRT1 (0.4 ± 0.1 vs. 0.8 ± 0.2; $t = 4.382$, $p < 0.01$) decreased (Figure 4); the expression of SIRT1 protein (0.3 ± 0.05 vs. 0.8 ± 0.2; $t = 5.941$, $p < 0.01$) decreased (Figure 5, a and c).

3.4. Effect of HCV core protein on activity and expression of AMPK

Compared to mock-transfected HepG2 cells, the activity of AMPK (0.3 ± 0.1 vs. 0.9 ± 0.3; $t = 4.648$, $p < 0.01$) in HepG2 cells expressing HCV core protein decreased (Figure 3); the mRNA levels of AMPKα2 (0.2 ± 0.05 vs. 0.9 ± 0.3; $t = 5.715$, $p < 0.01$) decreased (Figure 4); the expression of p-AMPK protein (0.1 ± 0.02 vs. 0.5 ± 0.1; $t = 9.608$, $p < 0.01$) decreased (Figure 5, b and c). There was no difference in the expression of AMPK protein between the two cell populations (0.7 ± 0.2 vs. 0.6 ± 0.3; $t = 0.679$, $p > 0.05$).

3.5. Effect of HCV core protein on glucose uptake and glucose production

Glucose uptake in HepG2 cells expressing HCV core protein was significantly lower than that of mock-transfected HepG2 cells (count per minute (cpm) 4600 ± 500 vs. $21\,000 \pm 4600$; $t = 8.682$, $p < 0.01$). HepG2 cells expressing HCV core protein produced greater amounts of glucose than did the control cells (2.6 ± 0.7 vs. 1.0 ± 0.1; $t = 5.543$, $p < 0.05$).

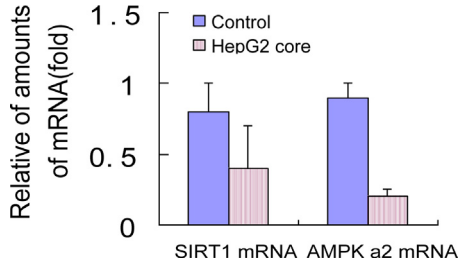

Figure 4. Effect of HCV core protein on the expression of SIRT1 and AMPKα2 mRNA. The expression levels of SIRT1 and AMPKα2 mRNA were measure by RT-PCR as described in the Materials and methods section. The results have been normalized to GAPDH and are expressed as the levels relative to control. The data shown are the means of six independent experiments (abbreviations: SIRT1, silent information regulator 1; AMPK, AMP-activated protein kinase).

3.6. Effect of HCV core protein on mRNA levels of glucose metabolism-related genes

The GLUT2 mRNA level in HepG2 cells expressing HCV core protein was significantly lower than that of mock-transfected HepG2 cells (0.4 ± 0.1 vs. 1 ± 0.2; $t = 6.573$, $p < 0.01$). There was no significant difference in GLUT1 mRNA levels between the two cell populations (0.9 ± 0.3 vs. 1 ± 0.3; $t = 0.577$, $p > 0.05$) (Figure 6). Compared to mock-transfected HepG2 cells, GK mRNA levels in HepG2 cells expressing HCV core protein decreased (0.6 ± 0.1 vs. 0.9 ± 0.3; $t = 2.324$, $p < 0.05$), the PEPCK mRNA levels (2.8 ± 0.6 vs. 1.0 ± 0.3; $t = 6.573$, $p < 0.01$) and the G6Pase mRNA levels (2.6 ± 0.5 vs. 1.0 ± 0.2; $t = 7.278$, $p < 0.01$) increased (Figure 6).

3.7. Effect of HCV core protein on triacylglycerol and cholesterol contents

The intracellular TG content in HepG2 cells expressing HCV core protein was significantly higher than that of mock-transfected HepG2 cells (78.2 ± 18.5 vs. 42.3 ± 10.5 μg/mg; $t = 4.134$, $p < 0.01$). The intracellular cholesterol content in HepG2 cells expressing HCV core protein was significantly higher than that of mock-transfected HepG2 cells (52.6 ± 12.0 vs. 31.5 ± 8.7 μg/mg; $t = 3.487$, $p < 0.01$).

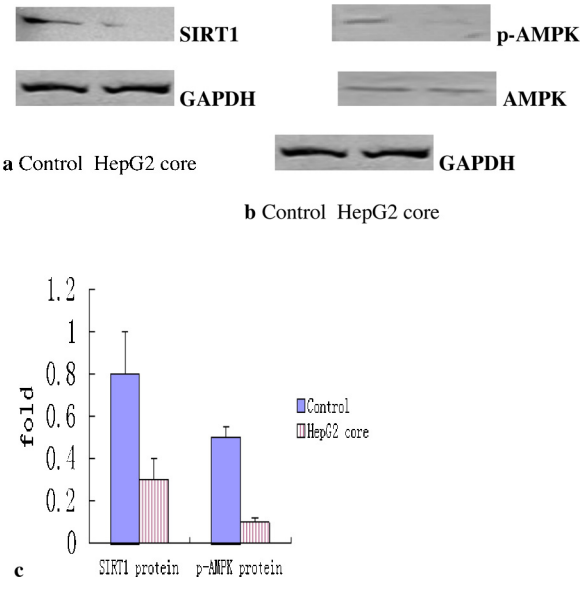

Figure 5. Effect of HCV core protein on the expression of SIRT1 and AMPK protein. (a) The expression of SIRT1 protein by Western blot. (b) The expression of AMPK and p-AMPK protein by Western blot. (c) Signal quantification by densitometry of SIRT1 and p-AMPK protein normalized to GAPDH expression. The expression levels of SIRT1 and AMPK protein were measured by Western blot as described in the Materials and methods section. The data shown are the means of six independent experiments (abbreviations: SIRT1, silent information regulator 1; AMPK, AMP-activated protein kinase; GAPDH, glyceraldehyde-3-phosphate dehydrogenase; p-AMPK, phospho-AMPK).

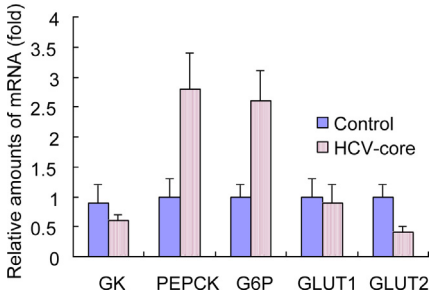

Figure 6. Effect of HCV core protein on mRNA levels of glucose metabolism-related genes. Transcriptional levels of glucose metabolism-associated genes were examined by real-time quantitative PCR. The results have been normalized to GAPDH and are expressed as the levels relative to control. Each data point represents the mean ± standard deviation of six individual experiments (abbreviations: GLUT, glucose transporter; G6P, glucose-6-phosphatase; GK, glucokinase; PEPCK, phosphoenolpyruvate carboxykinase).

3.8. Effect of HCV core protein on mRNA levels of lipid metabolism-related genes

As shown in Figure 7, compared to mock-transfected HepG2 cells, the SREBP-1c mRNA levels (1.8 ± 0.5 vs. 0.9 ± 0.3; $t = 3.781$, $p < 0.01$), the FAS mRNA levels (3.1 ± 0.5 vs. 1.0 ± 0.3; $t = 8.822$, $p < 0.01$), the ACC mRNA levels (2.5 ± 0.5 vs. 1.0 ± 0.2; $t = 6.823$, $p < 0.01$), the HMGR mRNA levels (1.8 ± 0.5 vs. 1.0 ± 0.2; $t = 3.639$, $p < 0.01$), and the HMGS mRNA levels (2.7 ± 0.6 vs. 1.0 ± 0.2; $t = 6.584$, $p < 0.01$) in HepG2 cells expressing HCV core protein increased; whereas the PPARα mRNA levels (0.3 ± 0.1 vs. 1.1 ± 0.3; $t = 6.197$, $p < 0.01$) and CPT1A mRNA levels (0.4 ± 0.1 vs. 1.0 ± 0.3; $t = 4.648$, $p < 0.01$) decreased. The PPARγ (0.9 ± 0.3 vs. 1.0 ± 0.2; $t = 0.679$, $p > 0.05$) and SREBP-2 mRNA levels (0.9 ± 0.3 vs. 1.0 ± 0.2; $t = 0.679$, $p > 0.05$) were similar in the two cell populations (Figure 7).

4. Discussion

Hepatic steatosis and insulin resistance caused by HCV infection are factors that aggravate the progression of liver disease. Although the pathogenesis of liver disease and metabolic disorders in HCV infection is poorly understood, oxidative stress due to mitochondrial respiratory chain dysfunction plays a pivotal role.

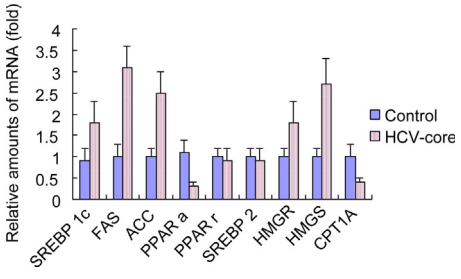

Figure 7. Effect of HCV core protein on mRNA levels of lipid metabolism-related genes. Transcriptional levels of lipid metabolism-associated genes were examined by real-time quantitative PCR. The results have been normalized to GAPDH and are expressed as the levels relative to control. Each data point represents the mean ± standard deviation of six individual experiments (abbreviations: PPAR, peroxisome proliferator-activating receptor; HMGR, HMG-CoA reductase; HMGS, HMG-CoA synthase; FAS, fatty acid synthase; CPT1, carnitine palmitoyl transferase 1, SREBP, sterol regulatory element binding protein; ACC, acetyl-CoA carboxylase).

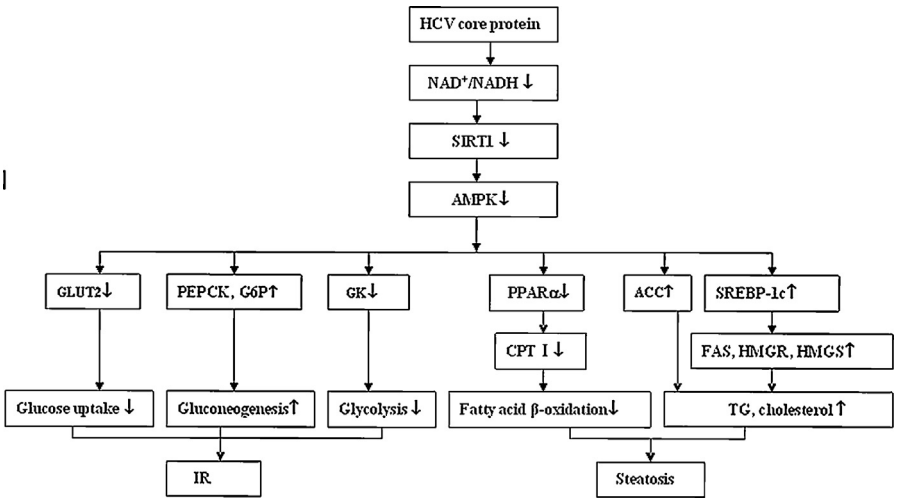

Figure 8. Schematic representation of the signaling pathway induced by HCV core protein for metabolism disorders of hepatocytes. HCV core protein induces the alterations in cellular redox state (the decrease in the NAD^+/NADH ratio) and could influence the activity of SIRT1 and secondarily AMPK, then change the expression profile of glucose and lipid metabolism-related genes, thereby causing metabolism disorders of hepatocytes. An arrowhead pointing upward (↑) represents activation and an arrowhead pointing downward (↓) represents the repression of activity.

Our results suggest that HCV core protein induces alterations in the energy state and redox state of hepatocytes: an increase in ROS production and decrease in the NAD^+/NADH ratio. These findings are consistent with those of Wang et al., who showed that HCV core protein caused dysfunction of the mitochondrial respiratory chain complex 1 and increased the ROS production or lipid peroxidation and decreased the NAD^+/NADH ratio in core gene transgenic mice and in HepG2 cells expressing the core protein.[10]

In the present study, we proved that the activity and abundance of AMPK significantly diminished in HepG2 cells expressing HCV core protein. There was no significant difference in ATP/ADP ratios between the two cell populations. Our results suggest that the observed changes in AMPK activity are not associated with alterations in cellular AMP/ATP ratios. Although the activation of AMPK appears to be a direct consequence of an increase in the AMP-to-ATP ratio in many situations, studies in various tissues have shown that AMPK can be activated or inhibited by mechanisms that may not involve changes in adenine nucleotide levels.[17] Some scholars have raised the possibility that alterations in its cellular redox state (the increase in NAD^+ levels) contributes to AMPK activation.[18] So the changes of AMPK caused by HCV infection may be linked to concomitant changes in SIRT1 abundance and activity.

The NAD^+-dependent deacetylase SIRT1 is a key regulator of several aspects of metabolism. Changes in the NAD^+/NADH ratio within a cell, i.e., the cellular redox state, may influence SIRT1 activity.[19] Changes in SIRT1 may regulate AMPK activity. Overexpression of SIRT1 has been found to increase the phosphorylation of AMPK and ACC, both in vivo and in vitro, by a reaction dependent on the AMPK kinase LKB1.[20,21] Suchankova et al.,[22] found that high glucose-induced changes in AMPK are linked to alterations in SIRT1 abundance and activity. We found that SIRT1 activity and abundance decreased after HCV infection. We speculate that HCV core protein-induced alterations in the cellular redox state (decrease in the NAD^+/NADH ratio) could influence the activity of SIRT1 and secondarily AMPK.

AMPK is a key regulator of both glucose and lipid metabolism in the liver.[23] Activation of AMPK suppresses SREBP-1c, SREBP-2, and their target genes (ACC and FAS, the rate-limiting enzymes of fatty acid synthesis; HMGR, the rate-limiting enzyme for cholesterol synthesis) expression in hepatocytes. Activation of AMPK also up-regulates gene expression of PPARα and its target gene (CPT1, the rate-limiting enzyme of fatty acid β-oxidation). In this study, we found that the transcriptional levels of genes related to fatty acid and TG biosynthesis (SREBP-1c, FAS, and ACC) and cholesterol biosynthesis (HMGR and HMGS) were significantly increased; the transcriptional levels of genes related to fatty acid uptake and β-oxidation (PPARα and CPT1) were markedly suppressed. Thus HCV core protein induced hepatic TG and cholesterol accumulation.

Hepatocytes play a crucial role in maintaining plasma glucose homeostasis by adjusting the balance between hepatic glucose production and utilization via the gluconeogenic and glycolytic pathways, respectively. Activation of AMPK represses gene expression of the PEPCK and G6Pase (the rate-limiting enzymes of gluconeogenesis), and increases gene expression of the GK (the rate-limiting enzyme of glycolysis). Glucose is transported into hepatocytes via GLUT2. Activation of AMPK increases the glucose uptake by up-regulation of GLUT2. In this study, we found that HCV core protein promoted gluconeogenesis via transcriptional up-regulation of the genes for PEPCK and G6Pase and decreased glycolysis via transcriptional down-regulation of the gene for GK, which may result in a high concentration of glucose in HCV-infected hepatocytes. We also found that HCV core protein suppressed cellular glucose uptake through down-regulation of cell surface expression of GLUT2.

In conclusion, our study suggests that HCV core protein induces alterations in cellular redox state (decrease in the NAD^+/NADH ratio), which could influence the activity of SIRT1 and secondarily AMPK, then change the expression profile of glucose and lipid metabolism-related genes, thereby causing metabolism disorders of hepatocytes (Figure 8). These findings lay a foundation for the investigation of SIRT1–AMPK signaling pathway activity as new target for anti-HCV therapy for CHC patients with insulin resistance and steatosis.

Funding: This study was supported in part by a grant from the Science and Technology Research Foundation of the Department of Education, Heilongjiang Province, China (No. 11541158).

Conflict of interest: No benefits in any form have been received or will be received from a commercial party related directly or indirectly to the subject of this article.

References

1. Jian Wu Y, Shu Chen L, Gui Qiang W. Effects of fatty liver and related factors on the efficacy of combination antiviral therapy in patients with chronic hepatitis C. *Liver Int* 2006;**26**:166–72.
2. Yu JW, Sun LJ, Zhao YH, Kang P, Yan BZ. The effect of metformin on the efficacy of antiviral therapy in patients with genotype 1 chronic hepatitis C and insulin resistance. *Int J Infect Dis* 2012;**16**:e436–41.
3. Shaw RJ, Kosmatka M, Bardeesy N, Hurley RL, Witters LA, DePinho RA, et al. The tumor suppressor LKB1 kinase directly activates AMP activated kinase and regulates apoptosis in response to energy stress. *Proc Natl Acad Sci U S A* 2004;**101**:3329–35.
4. Horman S, Browne G, Krause U, Patel J, Vertommen D, Bertrand L, et al. Activation of AMP-activated protein kinase leads to the phosphorylation of elongation factor 2 and an inhibition of protein synthesis. *Curr Biol* 2002;**12**:1419–23.
5. Lochhead PA, Salt IP, Walker KS, Hardie DG, Sutherland C. 5-Aminoimidazole-4-carboxamide riboside mimics the effects of insulin on the expression of the 2 key gluconeogenic genes PEPCK and glucose-6-phosphatase. *Diabetes* 2000;**49**:896–903.
6. Mankouri J, Tedbury PR, Gretton S, Hughes ME, Griffin SD, Dallas ML, et al. Enhanced hepatitis C virus genome replication and lipid accumulation mediated by inhibition of AMP-activated protein kinase. *Proc Natl Acad Sci U S A* 2010;**107**:11549–54.
7. Nakashima K, Takeuchi K, Chihara K, Hotta H, Sada K. Inhibition of hepatitis C virus replication through adenosine monophosphate-activated protein kinase-dependent and independent pathways. *Microbiol Immunol* 2011;**55**:774–82.
8. Borradaile NM, Pickering JG. NAD(+), sirtuins, and cardiovascular disease. *Curr Pharm Des* 2009;**15**:110–7.
9. Cao C, Lu S, Kivlin R, Wallin B, Card E, Bagdasarian A, et al. SIRT1 confers protection against UVB- and H_2O_2-induced cell death via modulation of p53 and JNK in cultured skin keratinocytes. *J Cell Mol Med* 2009;**13**:3632–43.
10. Wang T, Campbell RV, Yi MK, Lemon SM, Weinman SA. Role of hepatitis C virus core protein in viral-induced mitochondrial dysfunction. *J Viral Hepat* 2010;**17**:784–93.
11. Banerjee S, Saito K, Ait-Goughoulte M, Meyer K, Ray RB, Ray R. Hepatitis C virus core protein upregulates serine phosphorylation of insulin receptor substrate-1 and impairs the downstream Akt/protein kinase B signaling pathway for insulin resistance. *J Virol* 2008;**82**:2606–12.
12. Kim KH, Hong SP, Kim K, Park MJ, Kim KJ, Cheong J. HCV core protein induces hepatic lipid accumulation by activating SREBP1 and PPAR gamma. *Biochem Biophys Res Commun* 2007;**355**:883–8.
13. Jiang WJ. Sirtuins: novel targets for metabolic disease in drug development. *Biochem Biophys Res Commun* 2008;**373**:341–4.
14. Gurd BJ, Yoshida Y, Lally J, Holloway GP, Bonen A. The deacetylase enzyme SIRT1 is not associated with oxidative capacity in rat heart and skeletal muscle and its overexpression reduces mitochondrial biogenesis. *J Physiol* 2009;**587**:1817–28.
15. Fujii N, Hirshman MF, Kane EM, Ho RC, Peter LE, Seifert MM, et al. AMP-activated protein kinase $\alpha 2$ activity is not essential for contraction- and hyperosmolarity-induced glucose transport in skeletal muscle. *J Biol Chem* 2005;**280**:39033–41.
16. Bligh EG, Dyer WJ. A rapid method of total lipid extraction and purification. *Can J Med Sci* 1959;**37**:911–7.
17. Beauloye C, Marsin AS, Bertrand L, Krause U, Hardie DG, Vanoverschelde JL, et al. Insulin antagonizes AMP-activated protein kinase activation by ischemia or anoxia in rat hearts, without affecting total adenine nucleotides. *FEBS Lett* 2001;**505**:348–52.
18. Frederich M, Balschi JA. The relationship between AMP-activated protein kinase activity and AMP concentration in the isolated perfused rat heart. *J Biol Chem* 2002;**277**:1928–32.
19. Sauve AA, Schramm VL. Sir2 regulation by nicotinamide results from switching between base exchange and deacetylation chemistry. *Biochemistry* 2003;**42**:9249–56.
20. Hou X, Xu S, Maitland-Toolan KA, Sato K, Jiang B, Ido Y, et al. SIRT1 regulates hepatocyte lipid metabolism through activating AMP-activated protein kinase. *J Biol Chem* 2008;**283**:20015–26.
21. Lan F, Cacicedo JM, Ruderman N, Ido Y. SIRT1 modulation of the acetylation status, cytosolic localization, and activity of LKB1: possible role in AMP activated protein kinase activation. *J Biol Chem* 2008;**283**:27628–35.
22. Suchankova G, Nelson LE, Gerhart-Hines Z, Kelly M, Gauthier MS, Saha AK, et al. Concurrent regulation of AMP-activated protein kinase and SIRT1 in mammalian cells. *Biochem Biophys Res Commun* 2009;**378**:836–41.
23. Hardie DG. AMP-activated/SNF1 protein kinases: conserved guardians of cellular energy. *Nat Rev Mol Cell Biol* 2007;**8**:774–85.